PFC/JA-96-43

Transport Studies in the Scrape-off Layer and Divertor of Alcator C-Mod

B. LaBombard, J.A. Goetz, I.H. Hutchinson, D. Jablonski[1], J. Kesner, C. Kurz[2], B. Lipschultz, G.M. McCracken[3], A. Niemczewski[4], J. Terry, A. Allen, R.L. Boivin, F. Bombarda,[5] P. Bonoli, C. Christensen, C. Fiore, D. Garnier, S. Golovato,[6] R. Granetz, M. Greenwald, S. Horne,[7] A. Hubbard, J. Irby, D. Lo, D. Lumma, E. Marmar, M. May,[8] A. Mazurenko, R. Nachtrieb, H. Ohkawa. P. O'Shea, M. Porkolab, J. Reardon, J. Rice, C. Rost, J. Schachter, J.A. Snipes, J. Sorci, P. Stek, Y. Takase, J. Terry, Y. Wang, R. Watterson,[9] J. Weaver[10] B. Welch,[10] S. Wolfe

October 1996

[1]presently at Defense Intelligence Agency, Washington, D.C., USA.
[2]presently at University of California, San Diego, CA, USA.
[3]presently at JET Joint Undertaking, Abingdon, UK.
[4]presently at McKinsey & Co., Inc., London, UK.
[5]Associazione Euratom-ENEA sulla Fusione, Frascati, Italy.
[6]presently at Tokyo Electron America, Beverly, MA, USA.
[7]presently at Applied Science and Technology, Inc., Woburn, MA, USA.
[8]The Johns Hopkins University, Baltimore, MD, USA.
[9]presently at CPClare Corporation, Lexington, MA, USA.
[10]University of Maryland, College Park, MD, USA.

To be published in the Proceedings of the 16^{th} IAEA Fusion Energy Conference.

This work was supported by the U. S. Department of Energy Contract No. DE-AC02-78ET51013.

F1-CN-64/AP2-5

TRANSPORT STUDIES IN THE SCRAPE-OFF LAYER AND DIVERTOR OF ALCATOR C-MOD

ABSTRACT

Parallel and cross-field heat and particle transport in the divertor and scrape-off layer (SOL) of Alcator C-Mod have been systematically studied using an extensive array of divertor/SOL diagnostics. Some key results include: (a) Classical parallel heat transport is obeyed with ion-neutral momentum coupling effects. (b) Cross-field heat transport is proportional to local gradients. (c) Cross field heat diffusivity is found to scale with local density, n, electron temperature, T_e, and magnetic connection length, L, approximately as $\chi_\perp \sim T_e^{-0.6}\, n^{-0.6}\, L^{-0.7}$ in ohmic L-mode discharges, insensitive to toroidal field strength. (d) $\chi_\perp$ depends on divertor neutral retention. (e) H-mode transport barrier effects partially extend into the SOL. (f) Thermoelectric currents in the SOL may play a role in forming inside/outside divertor asymmetries. (g) Reversed parallel flows in the SOL depend on inside/outside divertor asymmetries and may be caused by ionization source imbalances in the divertor legs.

1. PARALLEL HEAT TRANSPORT

Three different parallel heat transport regimes are routinely observed in the divertor/SOL which can coexist in the same discharge [1]: low-recycling, high-recycling (Fig.1a), and detached divertor (Fig.1b). The existence of low- and high-recycling regimes is consistent with classical parallel heat transport and localized volumetric losses in the divertor. As the divertor plasma density is increased, an accompanying increase in coulomb collisionality and divertor

radiation occurs while T_e gradients form along magnetic field lines, particularly near the strike point (0 mm in Fig.1) where radiation is high, field line lengths are long and power is additionally lost to the private flux zone.

Plasma detachment (pressure loss on a flux surface) is detected in regions in the divertor where the electron temperature at the divertor plate drops below ~ 5 eV. Neutral pressure measurements in the private flux zone and D_α emissivity measurements over the outer divertor surface confirm this region to be one of low ionization fraction (< 50%) where ion-neutral collisions become effective in removing and redistributing parallel plasma momentum. Fig. 1b shows an example of plasma detachment near the separatrix. The peak parallel heat flux at the entrance to the divertor region for this discharge is ~ 400 MW m^{-2}.

2. CROSS-FIELD SOL PROFILES

Figure 2 shows representative cross-field profiles of density, temperature, and electron pressure for three ohmic (L-mode) discharges with $\bar{n}_e$ = 1.3, 1.9, 2.5 x10^{20} m^{-3}, and one ELM-free H-mode discharge with $\bar{n}_e$ = 3.0x10^{20} m^{-3} (I_p = 1.0 MA, B_T= 5.3 tesla). All profiles display a non-exponential dependence on flux surface coordinate, i.e., the slope on the logarithmic plot varies substantially with location. The local pressure gradient scale lengths in ohmic (L-mode) plasmas can vary by a factor of ~ 4 across the profile and generally exhibit the smallest values at low density and largest values at high density. In contrast, depsite the higher core densities, H-mode plasmas exhibit the shortest pressure gradient scale lengths at the separatrix with over a factor of 10 variation across the profile (~1 mm at ρ = 0 to ~ 14 mm at ρ = 15 mm).

3. DEPENDENCE OF SOL GRADIENTS ON CORE CONFINEMENT

Pressure gradient scale lengths in the SOL are inversely correlated with the quality of the global energy confinement. Figure 3 plots the "H-factor" (global energy confinement time normalized to that from the ITER89P L-mode scaling law) versus the local electron pressure gradient scale length (λ_p) at the last closed flux surface (LCFS). Data are shown from a set of ohmic L-mode [2] and ICRF heated H-mode plasmas with a wide range of densities, currents and magnetic fields. These discharges were specially prepared for diagnosis with the scanning probe and therefore do not include the full range of H-factors accessible to Alcator C-Mod (up to ~2.5) [3]. The shortest pressure gradient scale lengths for any confinement regime tend to occur when the H-factor is highest. Ohmic H-modes exhibit a similar trend, having $\lambda_p <$ ~ 1mm.

4. SCALING OF LOCAL GRADIENT SCALE LENGTHS

For ohmic L-mode discharges, <u>local</u> cross-field pressure e-folding lengths in the SOL are found to scale with <u>local</u> plasma parameters over a wide range of discharge conditions ($0.5 < \bar{n}_e < 2.8\text{x}10^{20}$ m^{-3}, $0.4 < I_p < 1.1$ MA, $2.8 < B_T < 7.8$ tesla, attached/detached divertor). A power law formula for the perturbation of local λ_p about a mean value, λ_p^*, has been investigated [4],

$$\lambda_p = \lambda_p^* \, (T_e/50)^{\alpha} \, (n/10^{20})^{\beta} \, (L/12.5)^{\gamma} \, (B_T/5)^{\delta}, \qquad (1)$$

where: T_e, n - electron temperature (eV) and density (m^{-3}) at the scanning probe location, L - 1/2 of total connection length (m), B_T - toroidal magnetic field on axis (tesla). Results of regression analysis from a set of 130 discharges is shown in Table 1. The statistics of the data set is sufficient to separately resolve the dependence of λ_p on B_T and L. There is essentially no sensitivity of

λ_p to the magnitude of B_T, despite the factor of 2.5 variation of B_T in the data set.

*Table 1 - Regression analysis using Eq. (1). Multiple correlation coefficient (**R**) and sample variance (χ^2_R) determine the statistically best representation (gray column).*

λ_p^* (mm)	**2.36** ±.04	**2.37** ±.04	**2.48** ±.04	**2.34** ±.04	**2.48** ±.04
α	**-1.04** ±.03	**-1.13** ±.04	**-1.49** ±.06	**-1.15** ±.04	**-1.49** ±.06
β	_	**0.14** ±.04	**0.25** ±.04	**0.15** ±.04	**0.25** ±.04
γ	_	_	**0.72** ±.09	_	**0.73** ±.09
δ	_	_	_	**0.13** ±.07	**-.02** ±.07
R	**.877**	**.880**	**.899**	**.881**	**.899**
χ^2_R	**1.43**	**1.38**	**1.14**	**1.38**	**1.14**

The strong inverse dependence of local λ_p on local T_e is consistent with a model that balances classical parallel heat conduction with a level of anomalous cross-field transport that is proportional to the local pressure gradient ($\lambda_p \sim T_e^{-5/4}$) [1]. Based on this model, these data suggest that local cross-field heat diffusivity scales approximately as $\chi_\perp \sim T_e^{-0.6}\, n^{-0.6}\, L^{-0.7}$, with no explicit dependence on B_T.

5. ESTIMATES OF CROSS-FIELD HEAT DIFFUSIVITY PROFILES

A neutral leakage pathway (bypass) in the divertor structure was closed during the summer of 1995. The result was an increase in the divertor/midplane neutral pressure ratio from ~70 to ~ 250 in otherwise similar discharges. $\chi_\perp$

profiles (Fig. 4) deduced from an "onion skin" transport model [4] show a factor of ~3 variation over the SOL in L-mode discharges with the absolute level decreasing by a factor of ~3 when the bypass was closed. H-mode discharges show a large variation in $\chi_\perp$ across the SOL with values near the separatrix falling to ~0.1 $m^2\ s^{-1}$, perhaps indicative of the H-mode transport barrier extending partly into the SOL.

6. ASYMMETRIC HEAT AND PARTICLE TRANSPORT

6.1 Heat Transport Asymmetries

Low density discharges with a hot SOL (low collisionality) exhibit a large divertor asymmetry, having outside/inside electron temperature ratios approaching ~10 with negative B_T ($\mathbf{B}x\nabla B$ towards x-point) and ~0.2 with positive B_T (Fig.5a). The density and temperature asymmetry preserves nT_e ~ constant on a flux surface and suggests that a heat flux asymmetry which reverses (inside-outside) on reversal of B_T is responsible [5]. As the collisionality in the SOL increases, the magnitude of the asymmetry decreases, vanishing in the highest density (lowest edge temperature) discharges.

Measurements suggest that parallel heat fluxes arising from currents in the SOL significantly contribute to the total heat flux arriving at divertor surfaces. A large component of the current is thermoelectric in nature, i.e., consisting of parallel currents driven by the inside/outside temperature asymmetry and obeying classical conductivity. A runaway situation can occur: thermoelectric currents drive asymmetric inside/outside parallel heat fluxes which, in turn, cause an increased temperature asymmetry. This mechanism, which scales with SOL collisionality, may play an important role in forming divertor asymmetries [4].

6.2 Parallel Particle Flows

Reversed parallel plasma flows (away from the divertor surface) in the outer divertor leg are detected near the separatrix under conditions when the divertor temperature asymmetry favors a higher T_e in the outer divertor leg (case "A" with negative B_T in Fig. 5b). An imbalance in the ionization rate of neutrals in the private flux zone near the inner and outer strike points may influence the magnitude of flow at the Mach probe location and be responsible for the flow reversal [4]. Such an ionization imbalance may drive divertor-to-divertor parallel convection loops that encircle the entire core plasma.

[1] LABOMBARD, B., et al., Scaling and transport analysis of divertor conditions on the Alcator C-Mod tokamak, Phys. Plasmas **2** (1995) 2242-2248.

[2] GREENWALD, M., et al., Transport experiments in Alcator C-Mod, Phys. Plasmas **2** (1995) 2308-2313.

[3] TAKASE, Y., et al., IAEA-CN-64/A5-4, these Proceedings.

[4] LABOMBARD, B., et al., Experimental investigation of transport phenomena in the scrape-off layer and divertor, Plasma-Surface Interactions in Controlled Fusion Devices (Proc. Int. Conf., San Raphael, 1996), to be published in J. Nucl. Mater.

[5] HUTCHINSON, I. H., et al., The effects of field reversal on the Alcator C-Mod divertor, Plasma Phys. Control. Fusion **37** (1995) 1389-1406.

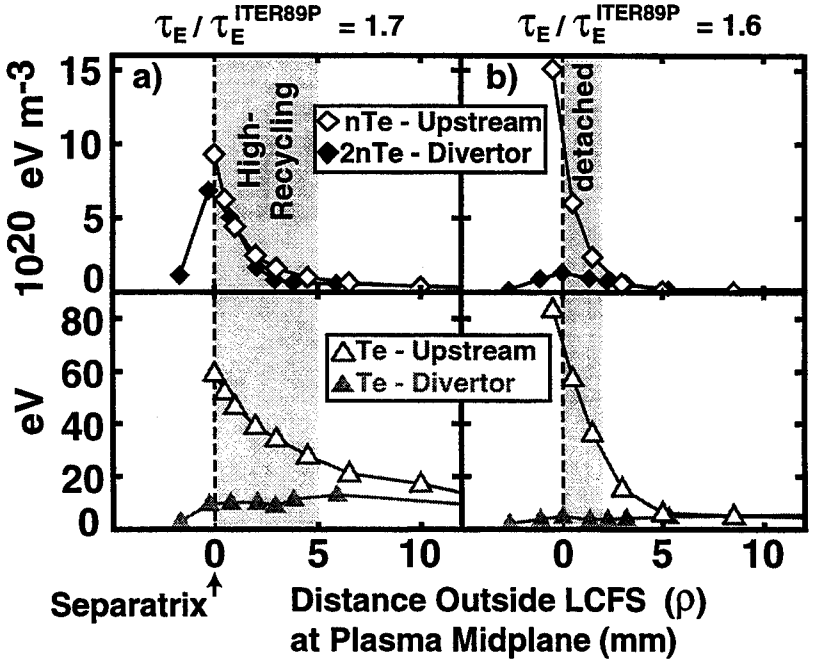

FIG. 1. Electron stagnation pressure and temperature profiles in H-mode plasmas recorded by a fast-scanning Langmuir-Mach probe upstream of the divertor throat and by divertor plate probes, mapped onto flux surface coordinate, ρ. a) Example of parallel T_e gradients forming in a high-recycling divertor discharge. b) Example of parallel T_e and nT_e gradients forming in a detached divertor discharge.

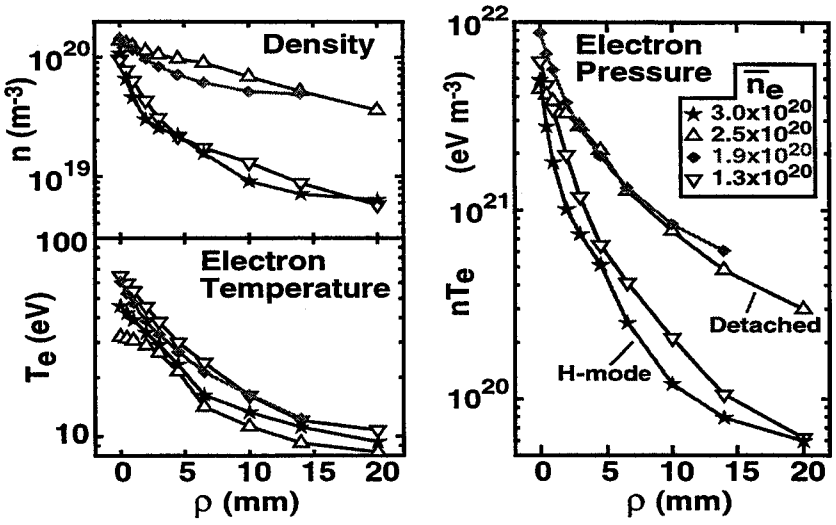

FIG. 2 Cross-field density and temperature profiles inferred from fast-scanning probe for different core line-averaged densities ($\bar{n}_e$). The steepest SOL pressure gradients appear near the separatrix in H-mode discharges.

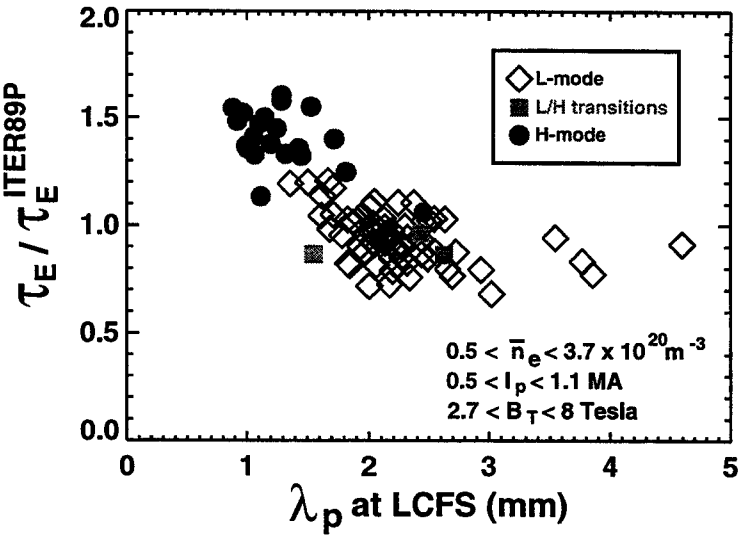

FIG. 3 Correlation between global confinement H-factor and electron pressure gradient scale length at the LCFS.

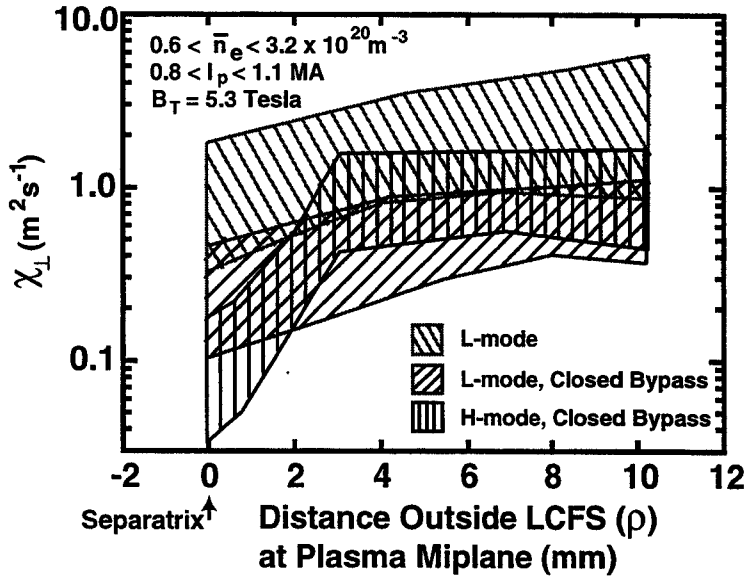

FIG. 4 Envelope of cross-field thermal diffusivity profiles, $\chi_\perp$, estimated from heat transport modeling of 93 diverted discharges.

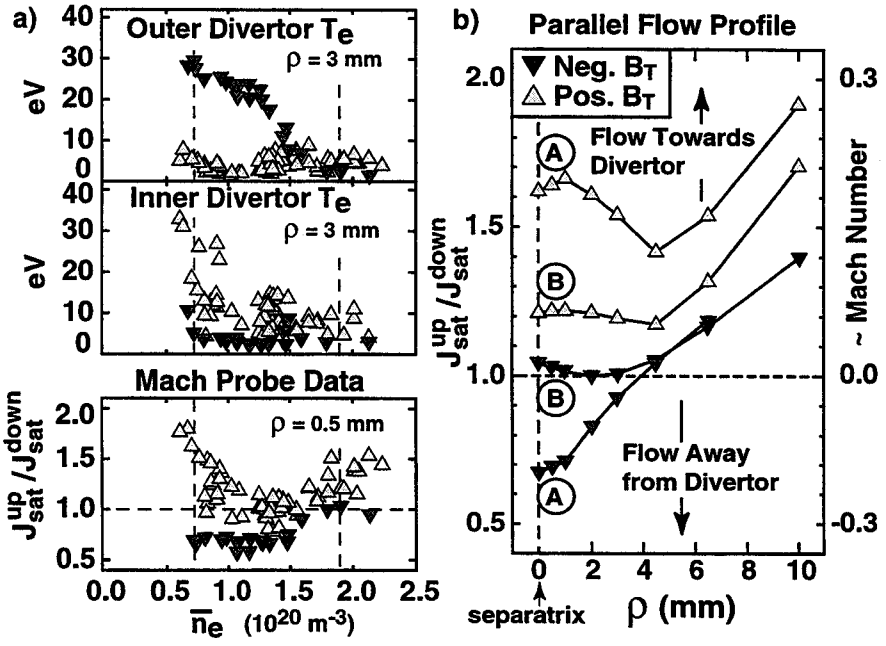

FIG. 5 (a) Outer and inner divertor T_e and ratio of ion saturation currents (J_{sat}) from a Mach probe (upstream of outer divertor leg) versus line-averaged density. Positive and negative field directions and flux surface location, ρ, is indicated. (b) Mach probe deduced parallel flow profiles for: (A) large in-out asymmetry, $\bar{n}_e = 0.7x10^{20}$ m^{-3} and (B) no asymmetry, $\bar{n}_e = 1.9x10^{20}$ m^{-3}.